IET Science, Measurement & Technology

Special Section: Selected Extended Papers from the International Conference on Computational Electromagnetics (CEM) 2019

IET Journals
The Institution of Engineering and Technology

Uncertainty identification method using kriging surrogate model and Akaike information criterion for industrial electromagnetic device

ISSN 1751-8822
Received on 1st August 2019
Revised 1st August 2019
Accepted on 18th February 2020
E-First on 18th March 2020
doi: 10.1049/iet-smt.2019.0349
www.ietdl.org

Saekyeol Kim[1], Soo-Gyung Lee[1], Ji-Min Kim[2], Tae Hee Lee[1] ✉, Myung-Seop Lim[1]

[1]*Department of Automotive Engineering, Hanyang University, Seoul 04763, Republic of Korea*

[2]*Digital Appliances, Samsung Electronics, Suwon 16677, Republic of Korea*

✉ *E-mail: thlee@hanyang.ac.kr*

Abstract: The uncertainty of an electromagnetic device is inherent in its manufacturing process. To consider the various uncertainties, several probabilistic design optimisation techniques, such as robust or reliability-based design optimisation, have been developed. Although a statistical model of uncertainties is extremely important in obtaining an accurate result from a probabilistic design optimisation, most studies on probabilistic design optimisation have assumed these uncertainties to follow normal distributions. However, this assumption may not be valid in several real-world applications. Therefore, this study presents an efficient uncertainty identification method that provides a systematic framework to select the fittest distribution and find its optimal statistical parameters using finite element analysis and experimental data from prototype testing. The Akaike information criterion and maximum likelihood estimation are used for model selection and parameter estimation, respectively. To reduce the computational cost, the kriging surrogate model is used to evaluate the response of the electromagnetic device. The proposed method is applied to a surface-mounted permanent magnet synchronous motor, to identify the uncertainties that produce the additional harmonic components of cogging torque. The results show that this method is a powerful tool in analysing the effect of uncertainties on the performance of an electromagnetic device.

1 Introduction

Mass-produced products usually exhibit variations in their characteristics and performances, owing to the presence of various uncertainties. In the worst-case scenario, this phenomenon can even lead to the production of defective products. These uncertainties generally arise from the manufacturing process and material properties. To improve the robustness and ensure the reliability of electromagnetic (EM) devices under various uncertainties, several probabilistic design optimisation techniques, such as robust design optimisation (RDO) and reliability-based design optimisation (RBDO), have been developed [1–4]. The purpose of RDO is to find a less-sensitive optimal solution under uncertainties, which results in a minimal variance in performance, while satisfying all design constraints. In RBDO, the probability of satisfying design constraint for each response is evaluated through a reliability analysis during the optimisation process. RBDO, thus, finds an optimal design under uncertainties, which guarantees a minimum level of reliability for each response.

The electrical power steering (EPS) system is an important application of probabilistic design optimisation. EPS has become an attractive alternative to hydraulic power steering in vehicles, owing to its contribution to the reduction in weight and fuel consumption. The cogging torque is the torque generated due to the interaction between the permanent magnets of the rotor and stator slots of the electric motor. Reducing the cogging torque is the most crucial design objective for EPS motors because it directly affects vehicle handling performance. The cogging torque shows a high degree of variation due to several uncertainties originating from the manufacturing process [5, 6]. The stamping process leads to various uncertainties in the geometric parameters of the stator in the surface-mounted permanent magnet synchronous motor (SPMSM) used in EPS. Thus, a reliability-based RDO has been adopted to ensure the quality and design feasibility of the performances of an EPS system [7]. Irregularities from the stacking process of metal sheets and imprecise attachment between the permanent magnets and rotor core cause uncertainties in the skew angle of the SPMSM used in EPS. To consider these uncertainties in probability design optimisation, a space–time kriging surrogate model was proposed [8]. A parametric study of the various design parameters that affect the cogging torque of the SPMSM for EPS was also conducted to analyse the variations resulting from manufacturing tolerances [9].

Although several probabilistic design optimisation techniques, such as RDO and RBDO, have been developed and applied to EM devices, they are usually based on the assumption that uncertainties follow a normal distribution [1–5]. In addition, the standard deviation of these uncertainties is usually determined based on the designer's experience. Although non-normal distributions have also been considered in a few studies [5, 10], the assumption of the statistical model and its parameters has not been validated. Owing to the fact that these assumptions can cause significant errors in the probabilistic design optimisation results, the statistical model and its parameters should be carefully determined. However, the identification of these uncertainties originating from the manufacturing process is extremely challenging at the initial design stage.

This study presents an uncertainty identification method that involves a systematic framework to obtain statistical models and their parameters using finite element analysis (FEA) and physical experimentation. To reduce the computational cost of the simulation, design of experiment (DOE) techniques and a kriging surrogate model are employed to evaluate the response of an EM device. The proposed method utilises maximum likelihood estimation (MLE), which estimates the parameters of the statistical model so that the observed prototype data become the most probable outcome. To compare various probability distributions and find the fittest one, the Akaike information criterion (AIC) is adopted. The proposed method was applied to an SPMSM for EPS based on a simulation model and its prototype test data.

The remainder of the paper is organised as follows. In the next section, the cogging torque that occurs in the SPMSM is described. In Section 3, the analysis of variance (ANOVA) is performed to investigate the influence of each design parameter on the cogging torque of an SPMSM. In Section 4, the kriging surrogate modelling

Table 1 Specifications of SPMSM

Name	Unit	Value
power	W	450
no. of poles	—	6
no. of slots	—	9
diameter of stator	mm	85
diameter of rotor	mm	38.8
material of stator and rotor	50PN470 (POSCO PN series)	
material of the permanent magnet	NMX-36H (Hitachi NEOMAX series)	
skew	three-step skew	

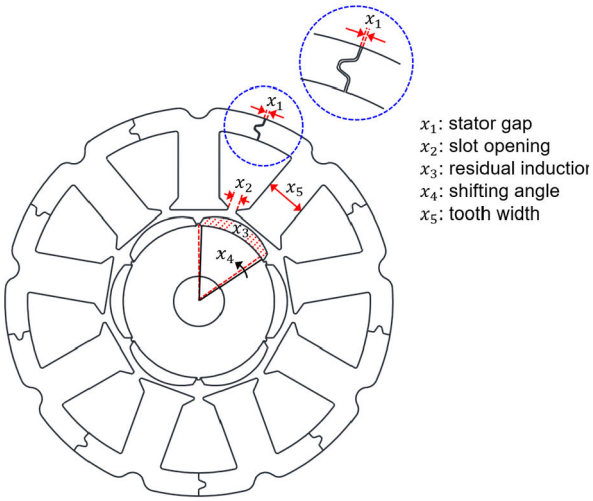

Fig. 1 *Stator and rotor cores of SPMSM*

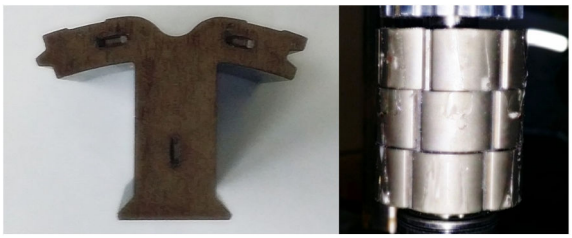

Fig. 2 *Manufactured prototypes of SPMSM. Note: From [2]. Copyright 2016 by IET Electric Power Applications (reproduced with kind permission from the IET)*

procedure is explained. Then, each step of the uncertainty identification procedure is described in Section 5. The application results for the SPMSM are discussed in Section 6, and the conclusions from the study are presented in Section 7.

2 Cogging torque of SPMSM

The cogging torque is an undesired effect that occurs owing to the interaction between the rotor magnets and stator slots. Owing to the stator slotting, the air-gap length varies periodically. This leads to a permeance change at the air gap and causes a periodic oscillation in the magnetic energy. Thus, a pulsating torque is generated, even at no-load operation. The cogging torque is a periodic function that can be obtained as a sum of the interactions between each edge of the rotor and stator slot openings. The harmonic components of the cogging torque can be divided into two different components according to their origin. The native harmonic components (NHCs) of the cogging torque are inevitable even in an ideal motor and always exist. The NHCs of the cogging torque can be easily evaluated through an FEA. The additional harmonic components (AHCs) of the cogging torque are usually generated in manufactured motors, owing to various uncertainties. Owing to the fact that AHCs are unpredictable at the initial design stage and are considered negligible, reducing the NHCs is usually the main design objective.

One of the most common strategies for reducing cogging torque is to apply a skew up to the value of a period of the cogging torque. The main harmonic order n_{mh} of the cogging torque can be calculated using the least common multiple of the magnetic poles and the number of the teeth on the stator, as follows:

$$n_{\mathrm{mh}} = \mathrm{LCM}(Q, P) \tag{1}$$

where Q is the number of slots in the stator and P is the number of poles in the rotor. Therefore, the orders of the NHC ($N_{\mathrm{NHC}i}$) that appear in the cogging torque is a multiple of the main harmonic order

$$N_{\mathrm{NHC}i} = n_{\mathrm{mh}} \cdot i \; (i = 1, 2, 3, \ldots) \tag{2}$$

Owing to the fact that the magnitude of the cogging torque decreases considerably as the order increases, eliminating the first few multiples of the main harmonic order is essential. The elimination of these harmonic components can be achieved by applying a skew angle to the rotor core. The orders of the remaining NHCs ($N_{\mathrm{NHCR}i}$) are determined by the number of steps applied

$$N_{\mathrm{NHCR}i} = n_{\mathrm{mh}} \cdot N_{\mathrm{S}} \cdot i \; (i = 1, 2, 3, \ldots) \tag{3}$$

where N_{S} is the number of steps.

The specifications and shape of the SPMSM for EPS used in this study are listed in Table 1 and shown in Fig. 1, respectively. Five design parameters were used for the uncertainty identification: stator gap, slot opening, residual induction and shifting angle of one magnet of the rotor, and tooth width. This model had six poles, nine slots, and included a three-step skew rotor. Therefore, the cogging torque occurred 18 times for each rotation. Owing to the three-step skew, 18th and 36th harmonic orders of cogging torque were eliminated, while the 54th harmonic order remained. The harmonic components that had a harmonic order larger than the 54th-order, were not considered because their effect is negligible. As the three-step skew was applied, the magnitude of the cogging torque reduced from 24.2 to 0.5 mNm [9].

To verify the cogging torque in the current design, six prototypes were manufactured. The manufactured stator and rotor prototypes are shown in Fig. 2. Owing to the fact that a divided core was applied, the size of the SPMSM could be reduced owing to a higher fill factor and shorter end-turn length, and the productivity could be increased because of the easier winding. The cogging torque of the prototype motors was measured using a torque sensor as shown in Fig. 3*a*. The results of the measurement were validated through a second measuring experiment using additional equipment, as shown in Fig. 3*b*. The validation in the previous study showed that the measured cogging torque of the six prototypes was considerably reliable [9]. The results of the harmonic analysis of the measured cogging torque are presented in Fig. 4. The magnitudes of the 6th and 9th harmonic orders of AHCs, which were expected to be eliminated, were particularly large and significantly contributed to the increase in the cogging torque. As the magnitude of the cogging torque of an SPMSM for EPS should be kept as low as possible, the AHCs cannot be neglected. To identify the effects of manufacturing uncertainties on the generation of AHCs, a parametric study was performed for this SPMSM [9]. The limitations of the previous study are that only the effect of certain levels of manufacturing tolerance were explored and the uncertainties were neither identified, nor quantified.

3 ANOVA for cogging torque

To investigate the influence of each design parameter on the cogging torque of the SPMSM in a systematic manner, the ANOVA was adopted. ANOVA has been widely employed for the design optimisation of EM systems [11, 12]. ANOVA is a form of statistical hypothesis testing that is widely used in the analysis of

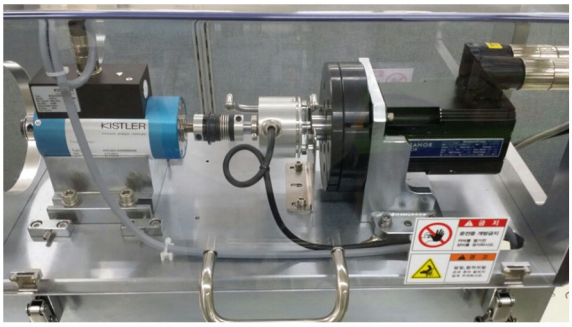

a

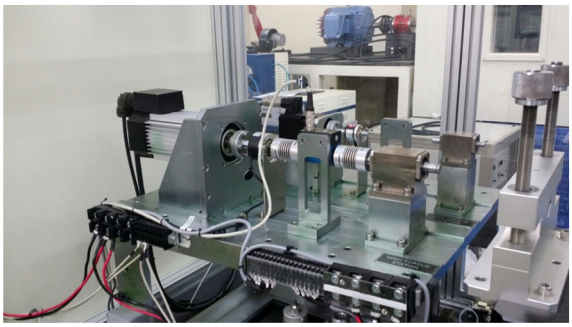

b

Fig. 3 *Measuring equipment for cogging torque*
(a) Primary equipment, ***(b)*** Additional equipment. Note: From [2]. Copyright 2016 by IET Electric Power Applications (reproduced with kind permission from the IET)

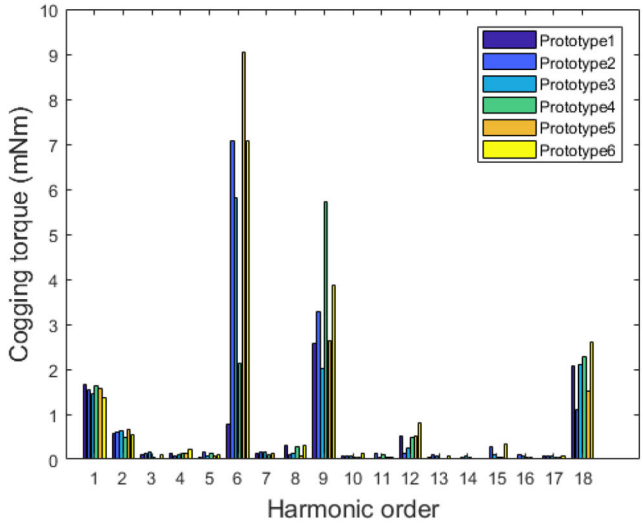

Fig. 4 *Experimental results of harmonic analysis of the measured cogging torque*

Table 2 Boundary of design parameters

Name	Description	Unit	L_1	L_2	L_3
x_1	stator gap	mm	0	0.05	0.1
x_2	slot opening	mm	1.9	2.0	2.1
x_3	residual induction	T	1.14	1.2	1.26
x_4	shifting angle	deg.	0	0.5	1
x_5	tooth width	mm	8.8	9.0	9.2

experimental data [13]. There are two hypotheses: the null hypothesis and the alternative hypothesis. In a typical application, the null hypothesis states that certain design factors do not have a significant influence on the response. On the contrary, the alternative hypothesis states that certain design factors are significant to the response. A DOE is usually performed to explore the change in response as design parameters are changed according to a pre-defined combination of certain levels. After the evaluation of the response at all design points, an F-test is performed for each design parameter. An F-test is used to assess whether the mean response values of a design parameter within pre-defined levels differ from each other. The test statistic in an F-test is the ratio of two-scaled sums of squares: one that reflects the variance caused by the level change in a design parameter and another that reflects the variance that is not explained by the changes in the design parameters. The test statistic tends to be greater when the null hypothesis is not true. The assessment can also be conducted by calculating the p-value of a value of F greater than or equal to the observed value. The null hypothesis is rejected if this probability is less than or equal to the pre-defined significance level α. The significance level of the test is usually chosen as 0.05, 0.01, or 0.001. The lower the significance level is, the more significant are the variables that the test selects.

In this study, the influences of the five design parameters were investigated. These design parameters were chosen based on the results of the parametric study in the previous work [9] and the discussion with design experts of EM device. Although various DOE techniques for ANOVA exist, an orthogonal array (OA) is employed in several cases owing to its simplicity and efficiency [14, 15]. Therefore, a three-level OA table that consists of 18 experiments was adopted. Table 2 presents the boundary of design parameters and Table 3 is the three-level OA table with the corresponding sixth-order and ninth-order AHC values of cogging torque. Owing to the fact that a small number of manufacturing uncertainties generated the AHCs of cogging torque, the p-value was determined as 0.001 in order to select the most significant design parameters.

Tables 4 and 5 list the results of the ANOVA for the cogging torque. The stator gap was the dominant design parameter that significantly affected the sixth-order AHC. The ninth-order AHC was mainly influenced by the residual induction and the shifting angle of the magnet position.

4 Surrogate model

Before we embark upon identifying and quantifying these uncertainties, it will be necessary to briefly understand surrogate modelling. A surrogate model is a functional relationship between the design parameter domain and response, which is widely used in the design optimisation of EM devices, to reduce the large computational cost associated with computer simulation [16, 17]. As an extremely large number of evaluations of the computer simulation are required, the construction of a surrogate model for the sixth-order and ninth-order AHCs is necessary. A general surrogate modelling procedure consists of three main stages: DOE, surrogate modelling and validation of the surrogate model. There are several options for each step, which can be selected according to the characteristics of the problem, the computational cost, comfortability and accuracy. However, the details regarding the theory or comparative study are beyond the scope of this paper. Therefore, a brief explanation of the selected methodologies and their numerical results will be provided along with some popular references.

4.1 Design of experiment

The DOE is the sampling plan in the design parameter domain. The sampling strategy for constructing a surrogate model based on response data collected from deterministic computer simulations differs from that for real-world experimentation [18, 19]. Numerous DOE techniques and their combinations have been developed, and they are usually required to satisfy the following properties: granularity, space-filling, good projective or non-collapsing property and orthogonality [20].

In this study, uniform sampling was used for a one-dimensional design domain because the aforementioned properties could be easily satisfied. For the one-dimensional uniform sampling, the design domain was divided into ten intervals, by 11 sample points. For a two-dimensional design domain, a combination of optimal Latin hypercube design (OLHD) and sequential maximin distance design (SMDD) was adopted [15]. The objective of the OLHD was

Table 3 OA table for ANOVA of cogging torque

No.	Stator gap	Slot opening	Residual induction	Shifting angle	Tooth width	AHC sixth, mNm	AHC ninth, mNm
1	1	1	1	1	1	0.0007	5.6068
2	1	2	2	2	2	0.0010	3.6546
3	1	3	3	3	3	0.0042	9.7025
4	2	1	1	2	2	6.5443	6.5608
5	2	2	2	3	3	6.7463	7.0959
6	2	3	3	1	1	6.8143	5.9408
7	3	1	2	1	3	9.4959	0.0002
8	3	2	3	2	1	9.8666	6.7761
9	3	3	1	3	2	9.3514	8.9311
10	1	1	3	3	2	0.0018	9.5888
11	1	2	1	1	3	0.0029	5.6262
12	1	3	2	2	1	0.0027	3.6985
13	2	1	2	3	1	6.6702	7.0719
14	2	2	3	1	2	6.8298	5.8744
15	2	3	1	2	3	6.5053	6.6378
16	3	1	3	2	3	9.8344	6.7168
17	3	2	1	3	1	9.3658	8.8476
18	3	3	2	1	2	9.5142	0.0005

Table 4 ANOVA results for the sixth-order of AHC

Source of variation	Sum of squares	Degree of freedom	Mean squares	*F* ratio	*p*-value
x_1	289.1180	2	144.5590	19,998.3400	0
x_2	0.0320	2	0.0160	2.2300	0.1777
x_3	0.2100	2	0.1050	14.5300	0.0032
x_4	0.0360	2	0.0180	2.5200	0.1500
x_5	0.0200	2	0.0100	1.4000	0.3071
error	0.0510	7	0.0070	—	—
total	289.4680	17	—	—	—

Table 5 ANOVA results for the ninth-order of AHC

Source of variation	Sum of squares	Degree of freedom	Mean squares	*F* ratio	*p*-value
x_1	5.9940	2	2.9969	11.3600	0.0063
x_2	0.8120	2	0.4059	1.5400	0.2793
x_3	53.6840	2	26.8418	101.7900	0
x_4	67.2850	2	33.6423	127.5700	0
x_5	0.9520	2	0.4761	1.8100	0.2332
error	1.8460	7	0.2637	—	—
total	130.5720	17	—	—	—

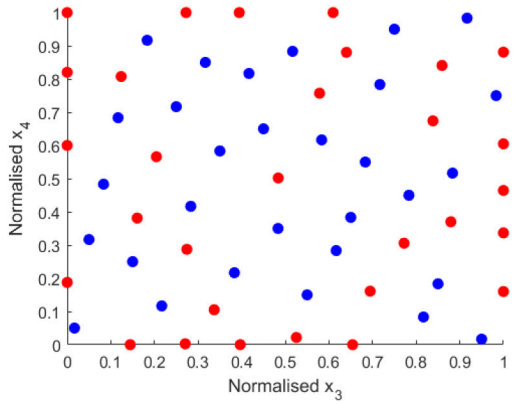

Fig. 5 *Sampling results in the two-dimensional normalised domain*

to obtain sample points that satisfy the space-filling and non-collapsing properties in the entire design domain [21]. The OLHD was first applied to obtain an initial set of 30 sample points. Then, the SMDD was performed by adding one sample point at one time, using the maximin distance criterion to guarantee sufficient information at the boundaries and an empty space in the design domain [22]. The SMDD was repeatedly performed until a total of 30 additional sample points were selected. Both sampling methods were applied in the normalised design domain in the range of [0, 1]. The sampling results obtained by using the combination of the OLHD and SMDD are illustrated in Fig. 5.

4.2 Kriging surrogate model

Several types of surrogate models are used in design optimisation: the response surface model, support vector machine, radial basis function, artificial neural network and kriging surrogate model [16, 17]. The response surface model is widely used because it is simple and is easy to apply. The support vector machine is a more complex regression model than the response surface model and fits the response in the design domain using the design samples from the DOE. These two models, however, assume that a random error exists in the sample data from the computer simulation. The radial basis function is a linear combination of weighted basis functions that interpolate the response data. The artificial neural network is also an interpolation model based on multiple hidden layers and

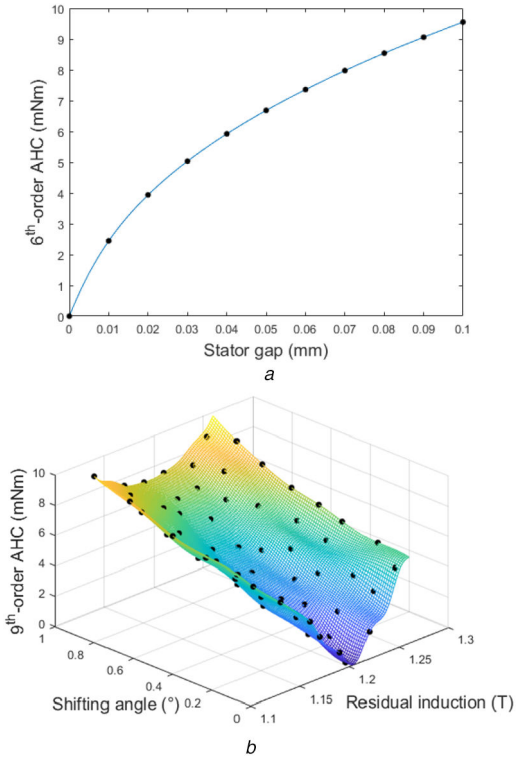

Fig. 6 *Sample set and kriging surrogate model for AHC*
(a) Sixth-order AHC, ***(b)*** Ninth-order AHC

hyperparameters. The disadvantages of these two models are that their accuracies highly depend on factors that should be defined by the users, such as the type of the basis function, the values of the model parameters, and the number of hidden layers. The kriging surrogate model is an interpolation model that covers the global trend of the response and local nonlinearity. The kriging surrogate model generally exhibits high accuracy for a non-linear response, using a reasonable number of samples from the DOE, and the model parameters are optimised by an MLE.

Although each model has its own advantages and disadvantages, all of them have been successfully employed in design optimisation. In this study, the kriging surrogate model was selected owing to its high accuracy for highly nonlinear functions and its highly reliable prediction capability [23, 24]. The kriging surrogate model is the sum of a global model and a local model and is expressed as [25–27]

$$\hat{\boldsymbol{Y}}(\boldsymbol{x}) = \boldsymbol{f}(\boldsymbol{x})^{\mathrm{T}}\hat{\boldsymbol{\beta}} + \boldsymbol{r}(\boldsymbol{x})^{\mathrm{T}}\boldsymbol{R}^{-1}\left(\boldsymbol{Y} - \boldsymbol{F}\hat{\boldsymbol{\beta}}\right) \tag{4}$$

where $\boldsymbol{f}(\boldsymbol{x})$ is the vector of known regression functions; $\hat{\boldsymbol{\beta}}$ is the estimator of the vector of unknown regression coefficients; $\boldsymbol{R}$ is the correlation matrix among the sampled design points; $\boldsymbol{r}(\boldsymbol{x})$ is the correlation vector between the sampled design points and prediction design point; $\boldsymbol{Y}$ is the response vector at the sampled design point and $\boldsymbol{F}$ is the expanded design matrix. The first component is the estimator of the global model and the second component is the deviation from the estimated mean model. The global model is determined by the generalised least squares method. The local model includes a correlation matrix, which is defined by a correlation function. In this study, ordinary kriging, which is the most commonly used form of kriging to the approximate computer simulation model, was employed [27]. A Gaussian correlation function is preferred and is widely used to construct a smooth response function, which is defined as

$$\boldsymbol{R}\left(\boldsymbol{\theta}, \boldsymbol{x}^i, \boldsymbol{x}^j\right) = \exp\left(\sum_{k=1}^{n_{\mathrm{d}}} -\boldsymbol{\theta}_k\left(x_k^i - x_k^j\right)^2\right) \tag{5}$$

where n_{d} is the dimension of the design space; $\boldsymbol{x}^i$ and $\boldsymbol{x}^j$ are the vectors of sampled points i and j, respectively and $\boldsymbol{\theta}$ is the correlation coefficient vector which is determined by the MLE. Fig. 6 shows the sample set and kriging surrogate model for the sixth-order AHC and ninth-order AHCs. It can be noted that the sixth-order AHC exhibits an increase as the stator gap increases. The ninth-order AHC is linearly dependent on the shifting angle, and it linearly increases as the residual induction changes from the initial value.

4.3 Validation of kriging surrogate model

The assessment of the surrogate model's quality is as important as the DOE and selection of the surrogate model. To assess the validity of the surrogate model, an error measure and validation method should be first determined. As the surrogate model is an approximation model, there is a difference between the response values calculated from the surrogate model and those from the simulation model. The error measure is a quantitative value that evaluates the accuracy or the quality of a surrogate model. The validation method deals with the calculation of this measure using the given sample data. One of the most popular approaches is the cross-validation method. The advantage of this method is that it provides a nearly unbiased estimation of the generalisation error, and the corresponding variance is reduced. The disadvantage is that it requires the construction of several surrogate models [17].

In this study, the normalised root mean square error (NRMSE) and leave-one-out cross-validation method were used. The NRMSE obtained by using leave-one-out cross-validation is defined as

$$\mathrm{NRMSE} = \sqrt{\frac{1}{n_{\mathrm{s}}}\sum_{i=1}^{n_{\mathrm{s}}}\left(\frac{\hat{\boldsymbol{Y}}_{-i}(x_i) - \boldsymbol{Y}(x_i)}{\max\left(\boldsymbol{Y}(\boldsymbol{x})\right) - \min\left(\boldsymbol{Y}(\boldsymbol{x})\right)}\right)^2} \times 100 \tag{6}$$

where $\hat{\boldsymbol{Y}}_{-i}(\boldsymbol{x}_i)$ is the predicted response at the ith design point obtained from the kriging surrogate model, which is constructed leaving out the ith sample from training; $\boldsymbol{Y}(\boldsymbol{x}_i)$ is the response at the ith design point calculated from the simulation model; max $(\boldsymbol{Y}(\boldsymbol{x}))$ and min $(\boldsymbol{Y}(\boldsymbol{x}))$ are the maximum and minimum response values, respectively, among those at the design points; and n_{s} is the number of sample points. The NRMSEs of the kriging surrogate model for the sixth and ninth-order AHCs were 0.6153 and 3.9824%, respectively. The constructed kriging surrogate models were considered to be sufficiently accurate to be implemented in uncertainty identification.

5 Uncertainty identification

In certain engineering applications, the probability distribution of the design parameters is known, whereas that of the response is unknown. Most probabilistic design optimisation techniques, such as RDO and RBDO, focus on how to predict the distribution of the response or its statistical parameters. Therefore, the knowledge of the probability distribution of the design parameters is a critical precondition to applying any of these optimisation techniques. However, there is inadequate literature associated with the identification of the probability distribution or estimation of the statistical parameters of input uncertainty. As direct measurement of input parameters in the prototype samples may not be possible or may be more difficult than the measurement of responses, the inverse problem identifying the probability distribution and estimating its statistical parameters from the response measurements is the one that is usually solved. This is known as uncertainty identification and can be widely implemented because the measurement data of responses can be obtained more easily. Conventional methods such as the perturbation method and Monte Carlo simulation, however, are less accurate because of their linearisation of the response or their computational requirements [28, 29].

This paper proposes an uncertainty identification method that is computationally more efficient, while also maintaining accuracy. The framework of the proposed method is described in Fig. 7.

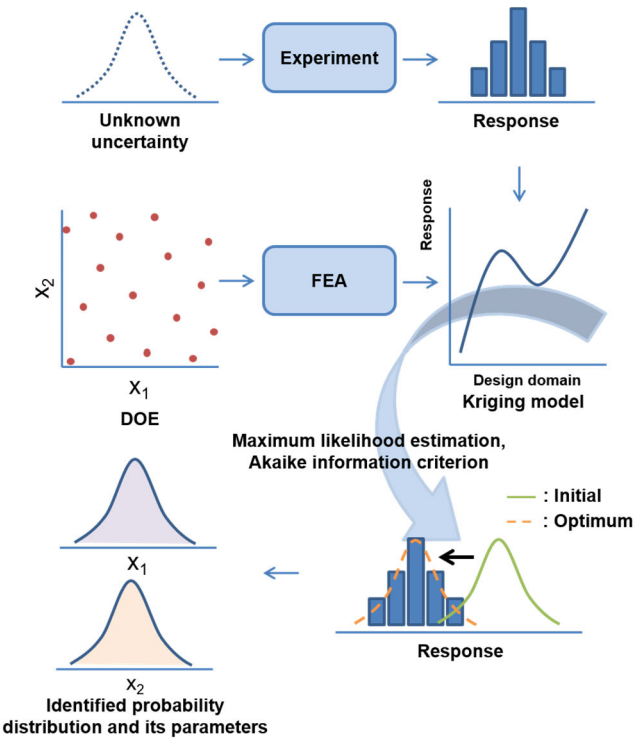

Fig. 7 *Framework of the uncertainty identification method*

First, the experimentation of the prototype samples is performed, and the response data are collected. Next, the kriging surrogate model is implemented to replace the simulation model that is constructed using response data from the FEA at design points determined by the DOE. To solve the inverse problem, the probability of the response should be obtained. The unknown probability distributions and the statistical parameters of the design parameters are first assumed based on the candidate distribution list and initial design. A total of 200 random samples are then generated, and the response data are evaluated using the kriging surrogate model. By using these data, the probability distribution of the response and its statistical parameters are determined using the AIC and MLE, respectively[30]. In this procedure, the experimental response data from six manufactured prototypes are used. A large sample size generally leads to increased accuracy and precision when estimating the unknown parameters of a distribution. The sample size is usually determined based on the available time and cost. Considering that only one or two prototypes are widely used for experimentation or design verification, the authors believe that the experimental data of six prototypes can yield a more reliable result.

For computational convenience and numerical stability, the natural logarithm of the likelihood is more commonly used instead of the likelihood function in the MLE. The log-likelihood is defined using the following equation:

$$l(\boldsymbol{\theta}) = \sum_{i=1}^{m} \log f(x_i; \boldsymbol{\theta}) \tag{7}$$

where l is the likelihood function; $\boldsymbol{\theta}$ is the statistical parameter vector of the distribution; f is the probability density function (PDF) of the distribution; m is the number of the data and x_i is ith datum.

The AIC is a quantified measure of the relative quality of the statistical models for the given data; it provides the fittest distribution among the candidate probability distributions by using the maximum value of the log-likelihood function and the number of statistical parameters. In doing so, it deals with the trade-off between the goodness of fit and the complexity of the model. The AIC is defined by the following equation:

$$\text{AIC} = -2\left(l_{\max} - n_{\text{p}}\right) \tag{8}$$

where $l_{\max}$ is the maximum log-likelihood value of the candidate distribution and n_{p} is the number of statistical parameters of each candidate distribution. The candidate distributions are usually selected by the design experts. As there is no prior knowledge about the response, six probability distributions that are widely implemented in various fields of science and engineering are chosen as follows: normal, log-normal, gamma, Weibull, minimum Gumbel and generalised extreme value (GEV) distributions. The normal, log-normal, and minimum Gumbel distributions have the location and scale parameters while the gamma and Weibull distributions have the scale and shape parameters. The GEV distribution has the location, scale and shape parameters.

After the probability distribution and its statistical parameters of the response are determined, MLE is applied using the response data from the experiment and the PDF of the response, to find the statistical parameters of the selected probability distribution of the design parameters. This procedure is repeatedly performed for all candidate probability distributions of the design parameters. When there is more than one uncertainty to identify, the combination of the assumed probability distributions is used. The candidate probability distributions for the unknown uncertainty of the design parameter are as follows: normal, log-normal, gamma, Weibull and maximum Gumbel distributions. The minimum Gumbel distribution was replaced by the maximum Gumbel distribution because a right-skewed distribution was not expected to be generated by the fabrication of the motor for the design parameter. The GEV distribution was also not included because the probability distribution of the uncertainty should not have an endpoint. The candidate probability distributions used in the proposed method are listed in Table 6. By comparing the log-likelihood function values obtained for each case, it is possible to quantify the quality of the identified probability distribution and select the most probable distribution with the maximum log-likelihood function value.

6 Application results

The proposed method was applied to identify the uncertainties of the design parameters of an SPMSM. Fig. 8 shows the application results for the sixth-order AHC of the cogging torque. It was found that there are two possible scenarios. The first case is that the stator gap was close to 0, as intended by the designer, and the frequency decreased as the stator gap became larger. The second case is that

Table 6 Candidate probability distributions

Name	PDF	Domain of definition	Parameters
normal	$f(x)=\frac{1}{\sqrt{2\pi\sigma^2}}\mathrm{e}^{\left((x-\mu)^2/2\sigma^2\right)}$	$-\infty<x<\infty$	$-\infty<\mu<\infty,\ -\infty<\sigma<\infty$
log-normal	$f(x)=\frac{1}{x\sqrt{2\pi\sigma^2}}\mathrm{e}^{\left((\ln x-\mu)^2/2\sigma^2\right)}$	$0<x<\infty$	$-\infty<\mu<\infty,\ -\infty<\sigma<\infty$
gamma	$f(x)=\frac{1}{\theta^{\alpha}\Gamma(k)}x^{k-1}\mathrm{e}^{-(x/\theta)}$	$0\le x<\infty$	$0<k<\infty, 0<\theta<\infty$
Weibull	$f(x)=\frac{k}{\lambda}\left(\frac{x}{\lambda}\right)^{k-1}\mathrm{e}^{-(x/\lambda)^k}$	$0\le x<\infty$	$0<\lambda<\infty, 0<k<\infty$
minimum Gumbel	$f(x)=\frac{1}{\sigma}\mathrm{e}^{\left(-\mathrm{e}^{((x-\mu)/\sigma)}+((x-\mu)/\sigma)\right)}$	$-\infty<x<\infty$	$-\infty<\mu<\infty, 0<\sigma<\infty$
maximum Gumbel	$f(x)=\frac{1}{\sigma}\mathrm{e}^{-\left(\mathrm{e}^{-((x-\mu)/\sigma)}+((x-\mu)/\sigma)\right)}$	$-\infty<x<\infty$	$-\infty<\mu<\infty, 0<\sigma<\infty$
GEV	$f(x)=\frac{1}{\sigma}\mathrm{e}^{\left(-(1+\xi((x-\mu)/\sigma))^{-(1/\xi)}\right)}\left(1+\xi\frac{(x-\mu)}{\sigma}\right)^{-1-(1/\xi)}$	$1+\xi\frac{(x-\mu)}{\sigma}>0$	$-\infty<\mu<\infty, 0<\sigma<\infty,\ -\infty<\xi<\infty$

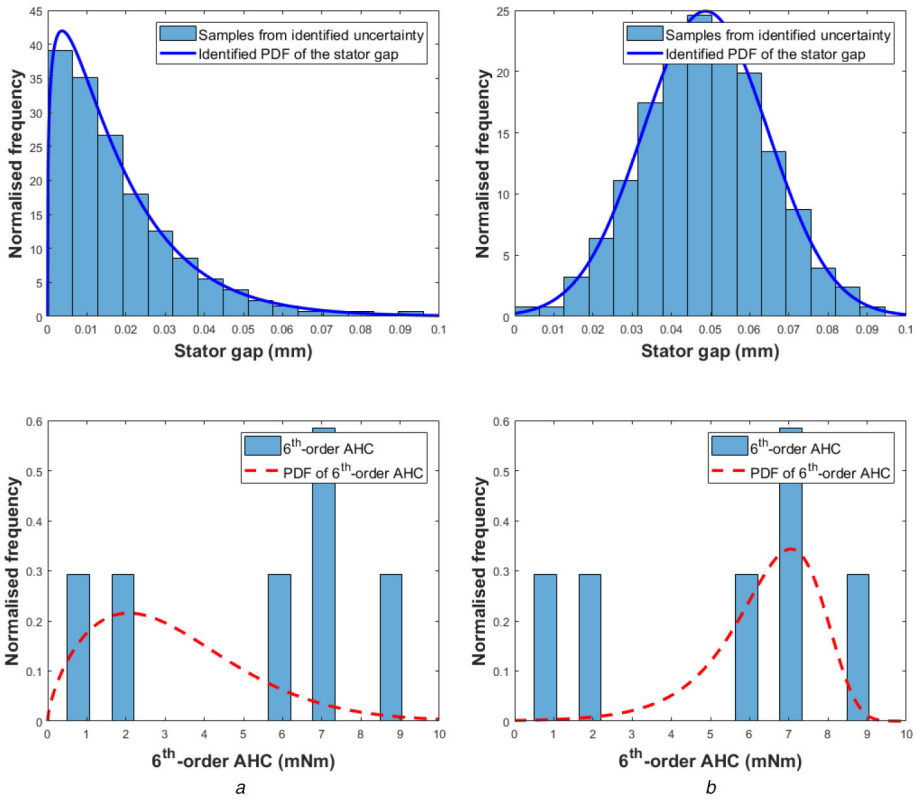

Fig. 8 *Application results for the sixth-order AHC*
(a) Case1: left-skewed distribution for response, ***(b)*** Case2: right-skewed distribution for response

the stator gap inevitably existed and followed a normal distribution. The probability distribution of the stator gap in the first case was identified as a gamma distribution with $k = 1.2550$ and $\theta = 0.0144$. The histogram in Fig. 8 represents the random sample set generated from this distribution. The identified uncertainty of the stator gap is reasonably acceptable because a large number of the products are designed to have a very small stator gap, close to 0. The probability distribution of the sixth-order AHC that maximises the log-likelihood function for the observed response data was the Weibull distribution with $\lambda = 3.5951$ and $k = 1.6664$. In the second case, the probability distribution of the stator gap was identified as a normal distribution with $\mu = 0.0487$ and $\sigma = 0.0160$. The probability distribution of the sixth-order AHC was identified as a minimum Gumbel distribution with $\mu = 7.0482$ and $\sigma = 1.0715$. This can also occur because the normal distribution is commonly used as a statistical model for manufacturing tolerance.

Although the results are the optimal solutions according to the proposed method and might be the possible scenarios, the observed cogging torque data has a slightly different trend compared with its PDF. There are three possible reasons for this phenomenon. First, the observed data were generated from one of the identified probability distributions and the identification results were correct. As the randomness cannot be controlled or predicted, there is always a possibility that the results from random samples seem to be a slightly different from those of the probability distribution, especially when the number of samples is small as in this case. Second, some critical design parameters that affect the generation of the sixth-order AHC were underestimated and should be considered. Last, the stator gap and sixth-order AHC of the cogging torque may not follow one of the candidate probability distributions. In this case, the statistical characteristics of the stator gap and the sixth-order AHC should be extensively studied and more candidate probability distributions should be added to obtain better results.

The application results for the ninth-order AHC are presented in Fig. 9. The probability distributions for the residual induction and shifting angle were identified as a maximum Gumbel distribution with $\mu = 1.1803$ and $\sigma = 0.0147$, and log-normal distribution with $\mu = -1.3029$ and $\sigma = 0.1459$ while the probability distribution of the ninth-order AHC was identified as a GEV distribution with $\mu =$

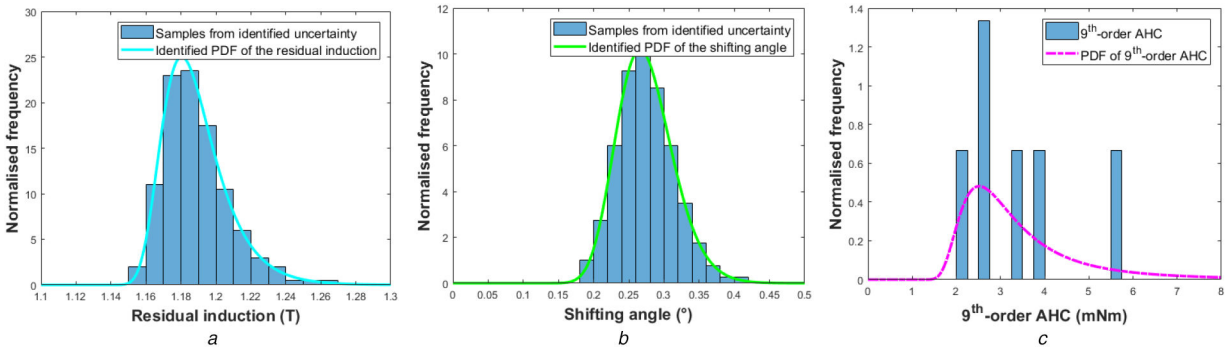

Fig. 9 *Application results for the 9th-order AHC*
(a) Uncertainty of residual induction, ***(b)*** Uncertainty of shifting the angle, ***(c)*** Ninth-order AHC

0.3230, $\sigma = 0.8012$, and $\xi = 2.7331$. It is important to note that the residual induction tended to be left-skewed while the position of the magnet was slightly shifted. The resulting PDF of the ninth-order AHC agreed very well with the experimental data.

7 Conclusion

This paper proposes an uncertainty identification method for uncertainties that are unknown, but inherent in the manufacturing process of industrial EM devices. This method consists of three steps. First, ANOVA is performed to investigate the influence of the design parameters and select the most significant ones to the response. Second, the kriging surrogate model is constructed by using DOE techniques and validated through leave-one-out cross-validation for each response. Finally, the AIC and MLE are employed to identify the probability distribution of the uncertainty and to optimise its statistical parameters using the experimental data. The major advantage of this method is that the computational time is largely reduced, which helps in dealing with non-linear characteristics of the response using the kriging surrogate model. In addition, any type of probability distribution can be considered by simply adding it in the list of candidate distributions.

To demonstrate the effectiveness of the proposed method, it was used to identify the uncertainties that caused unexpected cogging torque in an SPMSM for EPS. As a result, the stator gap was found to be the most significant design parameter of the sixth-order AHC. The probability distribution of the stator gap was identified as a gamma or normal distribution. The residual induction and shifting angle of the magnet, which were critical design parameters for the ninth-order AHC, were identified as a maximum Gumbel and log-normal distribution, respectively. The numerical results also show that even for extremely small manufacturing tolerances, the variability of material properties or misalignment of a component can cause a significantly large amount of the cogging torque in an SPMSM. To obtain more accurate and reliable results, more prototype samples are required, which will inevitably increase the development cost of the motor.

To the authors' best knowledge, this is a novel approach for systematically identifying the unknown uncertainties that occur in the manufacturing process of industrial products. The proposed method can offer a standard guideline for designers and engineers to utilise in the designing of EM devices, or to predict the potential problems of the current manufacturing process. The results of this study and the proposed method will contribute significantly for the improvement of more robust and reliable motors and reflect various uncertainties that exist in the real experiment.

8 References

[1] Kim, D., Jeung, G., Choi, K.K., *et al.*: 'Efficient strategies for reliability-based design optimisation of a superconducting magnetic energy storage system-based on reliability index approach', *IET Sci. Meas. Technol.*, 2013, **7**, (5), pp. 280–286

[2] Ren, Z., Zhang, D., Koh, C.: 'Investigation of reliability analysis algorithms for effective reliability-based optimal design of electromagnetic devices', *IET Sci. Meas. Technol.*, 2016, **10**, (1), pp. 44–49

[3] Kim, D., Kang, B., Choi, K.K., *et al.*: 'A comparative study on probability optimization methods for electromagnetic design', *IEEE Trans. Magn.*, 2016, **52**, (3), pp. 1–4, Art. no. 7201304

[4] Kang, B., Kim, D., Choi, K.K., *et al.*: 'Enriched performance measure approach for efficient reliability-based electromagnetic designs', *IEEE Trans. Magn.*, 2017, **53**, (6), pp. 1–4, Art. no. 7000604

[5] Gašparin, L., Černigoj, A., Markič, S., *et al.*: 'Additional cogging torque components in permanent-magnet motors due to manufacturing imperfections', *IEEE Trans. Magn.*, 2009, **45**, (3), pp. 1210–1213

[6] Coenen, I., Van der Giet, M., Hameyer, K., *et al.*: 'Manufacturing tolerances: estimation and prediction of cogging torque influenced by magnetization faults', *IEEE Trans. Magn.*, 2012, **48**, (5), pp. 1932–1936

[7] Jang, J., Cho, S., Lee, S., *et al.*: 'Reliability-based robust design optimization with kernel density estimation for electric power motor considering manufacturing uncertainties', *IEEE Trans. Magn.*, 2015, **51**, (3), pp. 1–4, Art. no. 8001904

[8] Jang, J., Lee, J.M., Cho, S., *et al.*: 'Space-time kriging surrogate model to consider uncertainty of time interval of torque curve for electric power steering motor', *IEEE Trans. Magn.*, 2018, **54**, (3), pp. 1–4, Art. no. 8200804

[9] Kim, J., Yoon, M., Hong, J., *et al.*: 'Analysis of cogging torque caused by manufacturing tolerances of surface-mounted permanent magnet synchronous motor for electric power steering', *IET Power Electron.*, 2016, **10**, (8), pp. 691–696

[10] Kang, B., Kim, D., Cho, H., *et al.*: 'Hybrid reliability analysis method for electromagnetic design problems with non-Gaussian probabilistic parameters', *IEEE Trans. Magn.*, 2017, **53**, (6), pp. 1–4, Art. no. 7000904

[11] Kim, S., Kim, C., Jung, S., *et al.*: 'Shape optimization of a hybrid magnetic torque converter using the multiple linear regression analysis', *IEEE Trans. Magn.*, 2016, **52**, (3), pp. 1–4, Art. no. 8102504

[12] Munoz, F., Alici, G., Li, W., *et al.*: 'Size optimization of a magnetic system for drug delivery with capsule robots', *IEEE Trans. Magn.*, 2016, **52**, (5), pp. 1–11, Art. no. 5100411

[13] Montgomery, D.C.: '*Design and analysis of experiments*' (John Wiley & Sons, USA, 2017, 9th edn.)

[14] Kim, S., Lim, W., Kim, H., *et al.*: 'Robust target cascading for improving firing accuracy of combat vehicle', *J. Mech. Sci. Technol.*, 2016, **30**, (12), pp. 5577–5586

[15] Kim, H., Kim, S., Kim, T., *et al.*: 'Efficient design optimization of complex system through an integrated interface using symbolic computation', *Adv. Eng. Softw.*, 2018, **126**, pp. 34–45

[16] Lei, G., Zhu, J., Guo, Y., *et al.*: 'A review of design optimization methods for electrical machines', *Energies*, 2017, **10**, (12), Art. no. 1962, pp. 1–31

[17] Queipo, N.V., Haftka, R.T., Shyy, W., *et al.*: 'Surrogate-based analysis and optimization', *Prog. Aerosp. Sci.*, 2005, **41**, (1), pp. 1–28

[18] Mckay, M.D., Beckman, R.J., Conover, W.J.: 'A comparison of three methods for selecting values of input variables in the analysis of output from a computer code', *Technometrics*, 2000, **42**, (1), pp. 55–61

[19] Kleijnen, J.P.C., Sanchez, S.M., Lucas, T.W., *et al.*: 'A user's guide to the brave new world of designing simulation experiments', *INFORMS J. Comput.*, 2005, **17**, (3), pp. 263–289

[20] Crombecq, K., Laermans, E., Dhaene, T.: 'Efficient space-filling and non-collapsing sequential design strategies for simulation-based modeling', *Eur. J. Oper. Res.*, 2011, **214**, (3), pp. 683–696

[21] Viana, F.A.C., Venter, G., Balabanov, V.: 'An algorithm for fast optimal Latin hypercube design of experiments', *Int. J. Numer. Meth. Eng.*, 2010, **82**, (2), pp. 135–156

[22] Johnson, M.E., Moore, L.M., Ylvisker, D.: 'Minimax and maximin distance designs', *J. Stat. Plan. Inference*, 1990, **26**, (2), pp. 131–148

[23] Lebensztajn, L., Marretto, C.A.R., Costa, M.C., *et al.*: 'Kriging: A useful tool for electromagnetic device optimization', *IEEE Trans. Magn.*, 2004, **40**, (2), pp. 1196–1199

[24] Wang, L., Lowther, D.A.: 'Selection of approximation models for electromagnetic device optimization', *IEEE Trans. Magn.*, 2006, **42**, (4), pp. 1227–1230

[25] Sacks, J., Welch, W.J., Mitchell, T.J., *et al.*: 'Design and analysis of computer experiments', *Stat. Sci.*, 1989, **4**, (4), pp. 409–423

[26] Lee, T.H., Jung, J.J.: 'Kriging metamodel based optimization', in Arora, J.S. (ed.): '*Optimization of structural and mechanical systems*' (World Scientific, Singapore, 2007), pp. 445–484

[27] Martin, J.D., Simpson, T.W.: 'Use of kriging models to approximate deterministic computer models', *AIAA J.*, 2005, **43**, (4), pp. 853–863

[28] Fonseca, J.R., Friswell, M.I., Mottershead, J.E., *et al.*: 'Uncertainty identification by the maximum likelihood method', *J. Sound Vib.*, 2005, **288**, (3), pp. 587–599

[29] Khodaparast, H.H., Mottershead, J.E., Friswell, M.I.: 'Perturbation methods for the estimation of parameter variability in stochastic model updating', *Mech. Syst. Signal Process.*, 2008, **22**, (8), pp. 1751–1773

[30] Akaike, H.: 'Information theory and an extension of the maximum likelihood principle', in Parzen, E., Tanabe, K., Kitagawa, G. (eds.): '*Selected papers of Hirotugu Akaike'* (Springer, USA, 1998), pp. 199–214